Int. J. Multiphase Flow Vol. 18, No. 3, pp. 465–473, 1992
Printed in Great Britain.

0301-9322/92 $5.00 + 0.00

BRIEF COMMUNICATION

STATISTICAL ANALYSIS OF WAVES IN HORIZONTAL STRATIFIED GAS–LIQUID FLOW

N. ANDRITSOS
Chemical Process Engineering Research Institute, P.O. Box 1517, Thessaloniki, 54006, Greece

(Received 12 September 1990; in revised form 20 October 1991)

INTRODUCTION

In a previous paper (Andritsos & Hanratty 1987a), the following subregions of the stratified gas–liquid flow in horizontal pipes were recognized:

1. A smooth region, occurring at very low gas and liquid velocities, where the gas–liquid interface is smooth.
2. A two-dimensional (2-D) wave region, where the interface is covered by regular two-dimensional waves as a result of pressure variations in phase with the wave slope (Jeffrey's sheltering hypothesis). Liquid viscosity affects considerably the initiation of these waves by shifting the transition toward higher gas velocities.
3. A Kelvin–Helmholtz (K–H) wave region with large amplitude, irregular waves associated with pressure variations in phase with the wave height (K–H instability), also known as roll waves. The transition to these waves is weakly influenced by both liquid viscosity and pipe diameter. As indicated by Andritsos *et al.* (1989) this mechanism is also responsible for the formation of slugs in medium and high viscosity liquids.
4. An atomization region, where droplets or liquid filaments are torn off from the crests of the K–H waves and deposited on the pipe wall. Specifically, the transition to this region is defined to be the point at which droplets are first observed on the top of the pipe. In addition, the liquid starts climbing up the walls of the pipe and for small pipe diameter and low viscosity liquids the shape of the interface is no longer approximated by a flat horizontal plane. It is noteworthy, however, that the behavior in this region is very similar to annular flow for large pipe diameters and high viscosity liquids, where most of the liquid flows at the bottom of the pipe. A summary of the theoretical tools used to explain the initiation of the various wave types is given by Hanratty (1983).

Transitions between the various subregions were presented in Andritsos & Hanratty (1987a) and Andritsos *et al.* (1989) for several liquid viscosities and for two pipe diameters, namely 2.52 and 9.53 cm. These transitions were identified visually, using criteria outlined in the above papers. The transition lines actually represent narrow transitional zones.

It is well-known that the different wave types exert an influence not only on the pressure drop of the system, but also on the mass and heat transfer rates both at the interface and at the pipe walls. A description of the nature of the waves is certainly useful in understanding the various flow patterns occurring in horizontal pipes.

This communication presents a statistical analysis of film thickness traces in the three stratified regions. It is shown that the waves in the 2-D and the K–H wave region are different with regard to their uniformity and regularity, while the waves in the K–H wave and atomization regions seem to possess similar features. The latter may support the notion that the K–H instability is responsible for the generation of the entrained liquid droplets (Tatterson *et al.* 1977).

EXPERIMENTAL

The apparatus used for collecting the film thickness traces is described by Andritsos & Hanratty (1987a). The film thicknesses were measured by a pair of parallel wire probes. This method is based on the fact that the conductance between two parallel wires increases linearly with the length of the immersion in a conductive solution. Two Plexiglas test sections were added to each pipeline to accommodate the parallel wire probes. The wires extended vertically across the entire pipe section and were kept vertical by attaching weights at the ends. The second probe was located 26.7 cm downstream from the first probe in the 9.53 cm dia pipe and 10.2 cm downstream in the small-diameter pipe.

To measure film heights the conductance probes were connected to an analyzer circuit. An oscillating signal (30 kHz) was sent to the probes and the analyzer converted the response to an analog signal. All the film height signals were digitized prior to their storage in a Digital LSI-11/23 microcomputer. Signal conversions and data analyses were carried out either by the aforementioned microcomputer or by a VAX-780 computer. Most of the film thickness data were sampled at a frequency of 250 Hz and the total number of points collected for each reported data point was 8000.

RESULTS AND DISCUSSION

Using time-series analysis various statistical parameters were calculated for a total of 70 points. The analysis included three liquid viscosities in the 2.52 cm pipe (1, 16 and 70 cP) and two viscosities for the 9.53 cm pipe (1 and 80 cP). An additional limited number of points was analyzed for a 4.5 cP liquid in the 2.52 cm pipe and for a 12 cP liquid in the large-diameter pipe. The estimated parameters are the mean film thickness, the standard deviation, the skewness and the flatness factors, the frequency, the wavelength and the amplitude of the waves.

The frequency of the waves may be obtained from the peak in the normalized auto-correlation function of the film thickness signal, from wave amplitude energy spectra and from the number of waves crossing a standard window. The peak in the normalized cross-correlation function of two film height signals provides the average time that is needed for a wave to travel from one probe to the other and, consequently, the average wave velocity. The above-mentioned functions are defined as in Bendat & Piersol (1971). The average wave height (twice the wave amplitude), Δh, is estimated from the standard deviation of the film height signal, σ,

$$\Delta h = 2\sqrt{2}\sigma,$$

and the wavelength from the values of wave velocity and the wave frequency.

Figures 1 and 2 present film thickness traces, auto- and cross-correlation functions for a low and an intermediate liquid viscosity, respectively. Each figure displays three cases at a constant liquid flow rate and increasing gas velocity. Cases 1(a) and 2(a) represent 2-D waves. These signals are characterized by well-defined periodicity, which is evident in both the auto- and cross-correlation functions. These functions retain their oscillatory character for long time delays (more than 10 wave periods), and they are symmetrical around the axis of time, as are the film traces with respect to the mean film thickness. This means that the waves maintain their spacings as they travel along the pipeline, or they propagate with apparently little change of the shape. The correlation coefficient of both functions approaches unity. The characteristic frequency of the waves can be easily deduced from the auto-correlation function, or from the energy spectrum, where the periodic waves produce a clear peak.

Figure 1(b) depicts a special case, a point on the transition zone between 2-D and K–H waves. The functions retain an oscillatory form, not as clear though as in the previous cases. Only the adjacent waves correlate well.

Figures 1(c), 2(b) and 2(c) are typical cases observed in the K–H and atomization region, which show a dramatic change in the nature of waves. Both correlation functions display a large degree of randomness. In these regions the wavelength is not regular, a consequence of the continuous change of the waves. Waves are seen either to coalesce with each other or to split as

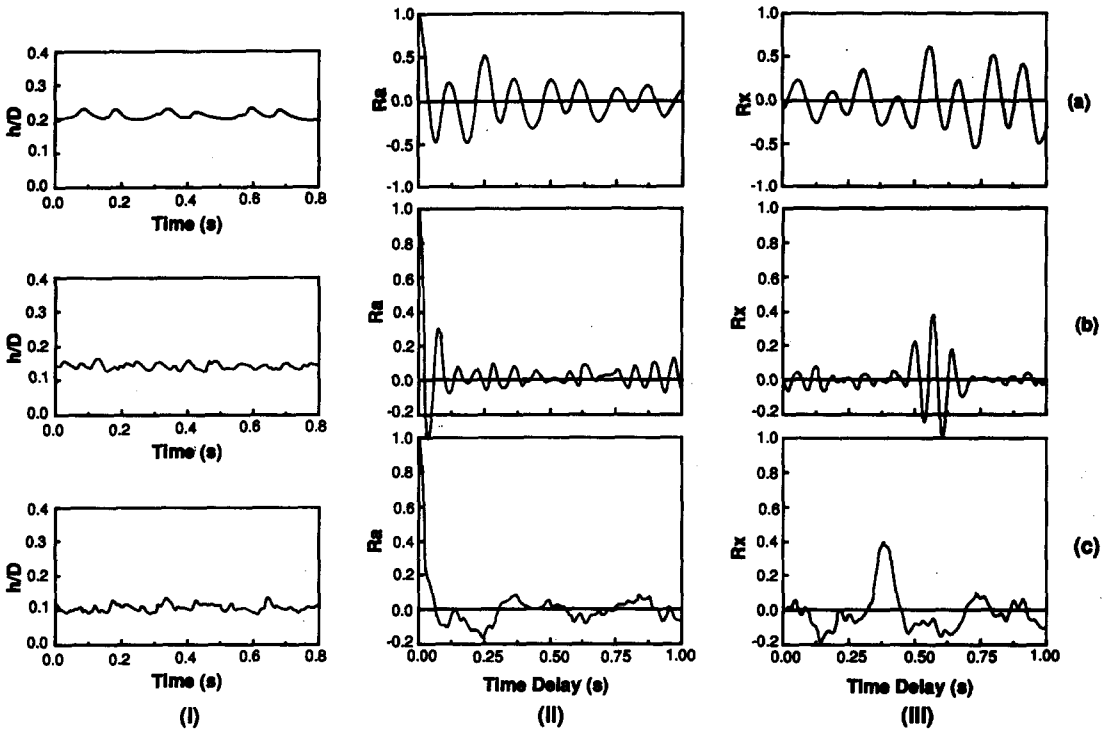

Figure 1. Film thickness traces (I), auto-correlation (II) and cross-correlation functions (III) for $D = 9.53$ cm, $\mu_L = 1$ cP, $U_{LS} = 0.025$ m/s and (a) $U_{GS} = 4.4$ m/s, (b) $U_{GS} = 6.8$ m/s and (c) $U_{GS} = 9.2$ m/s.

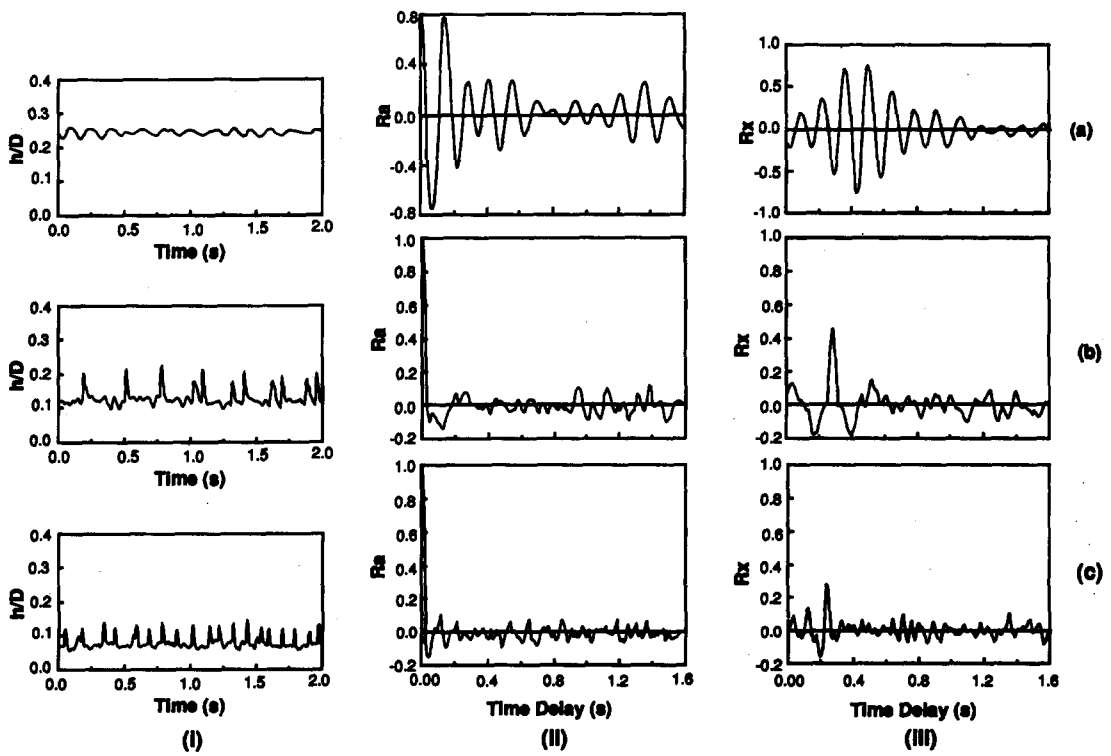

Figure 2. Film thickness traces (I), auto-correlation (II) and cross-correlation functions (III) for $D = 2.52$ cm, $\mu_L = 16$ cP, $U_{LS} = 0.007$ m/s and (a) $U_{GS} = 6.6$ m/s, (b) $U_{GS} = 9.4$ m/s and (c) $U_{GS} = 12.6$ m/s.

they travel along the pipe. Almost no information can be extracted from the auto-correlation function. For viscous liquids, the maximum located after the first minimum of the function may provide the characteristic period of the waves, but this is not clear for all cases and the use of the window crossing technique is required. Water represents a special case, since there are always small or large waves riding on low-frequency disturbances, as is clearly seen in the shape of the base film. In other words, the minima of the waves (troughs) do not lie on the same line as for the more viscous liquids. The characteristic period of the waves close to the transitional zone appears as a short peak, which by increasing the gas velocity takes the form of a "knee" in the auto-correlation function, as indicated by the arrow in figure 1(c). Thus, the estimation of the wave frequency from the auto-correlation function is quite enigmatic. The wave velocity, however, can be calculated easily from the cross-correlation function. A characteristic peak always appears, but the correlation coefficient is usually small and decreases with gas velocity, a sign of the continuous evolution of the wave shape. It is noted that for these conditions the distance between the two probes corresponds to about 2–6 wavelengths.

As mentioned previously, the frequency of K–H waves can be provided more accurately from the wave amplitude spectra than from the auto-correlation function. The window crossing technique can always be used to check both methods. This method is particularly convenient for the high viscosity liquids, where the waves are usually uniform in amplitude and the troughs are smooth. Typical spectra are shown in figures 3–5 for a high and a low viscosity liquid. Auto-correlation functions and wave traces around the mean are also included in these figures. The standard deviation of the film heights is indicated by the dashed lines.

Figure 3 shows the trace of a thin film ($h/D = 0.075$) for a 80 cP liquid in the 9.53 cm pipe and the corresponding power spectrum and auto-correlation function. It is evident that the waves are not periodic, although they seem to be quite uniform with respect to wave amplitude. Due to the non-periodicity of the waves, the auto-correlation function does not exhibit any well-defined peak. On the other hand, the waves produce a clear peak in the spectrum located at about 8 Hz. The number of waves in the 1 s film trace is 9, while window crossing of the film signal for a period of 20 s gave a frequency of 8.3 Hz. It is also of interest that the first peak of the auto-correlation function (in this case negative) gives a period about 0.12 s, or a frequency of 8.3 Hz. For higher film thicknesses (and higher wave frequencies) the wave amplitude is not as uniform as for small film heights, resulting in a rather flat spectrum.

A totally different picture appears in figures 4 and 5, where wave tracings, spectra and auto-correlation functions are displayed for water in a 9.53 and a 2.52 cm dia pipe, respectively. The interesting feature of both spectra is that they exhibit a rather flat region between 2 and 5 Hz and another clear peak, appearing at much higher frequencies (at 15 and 22 Hz, respectively). Obviously, this feature reflects the shape of the waves for water and for low viscosity liquids (< 5 cP) as can also be seen in the film traces. Small or large waves are seen riding on defined low-frequency disturbances. Wave spectra obtained for water and low viscosity liquids in horizontal channels exhibiting two peaks are also reported by Bruno & McCready (1989). It is noticeable that the "knee" in the auto-correlation functions corresponds to the characteristic frequency deduced from the second peak of the spectrum.

Values of wave velocity, C, wavelength, λ, wave height (non-dimensionalized using both the pipe diameter and the mean film thickness, $\Delta h/D$ and $\Delta h/h$, respectively), along with values of the flatness of the film height probability function are presented in tables 1 and 2 for the 9.53 cm dia pipe and for two liquid viscosities. The rest of the data can be found in Andritsos (1986). The ratio f_i/f_G is also included, since this quantity is a major design parameter and depends to a certain extent upon the type of wave region. Here, f_i is the interfacial friction factor and f_G is the friction factor corresponding to a smooth interface. The former is calculated from the momentum balance of the gas phase using measured pressure drop and film height data, while the latter is estimated by the Blasius equation (Andritsos & Hanratty 1987b).

In general, all quantities presented in the tables with the exception of the wave height change with gas velocity. Moreover, it is argued that certain quantities respond to the transition from the 2-D to K–H waves, although the scattered nature of the data does not allow for a definite conclusion. These quantities are the film thickness, the wave velocity, the flatness and the friction factor ratio.

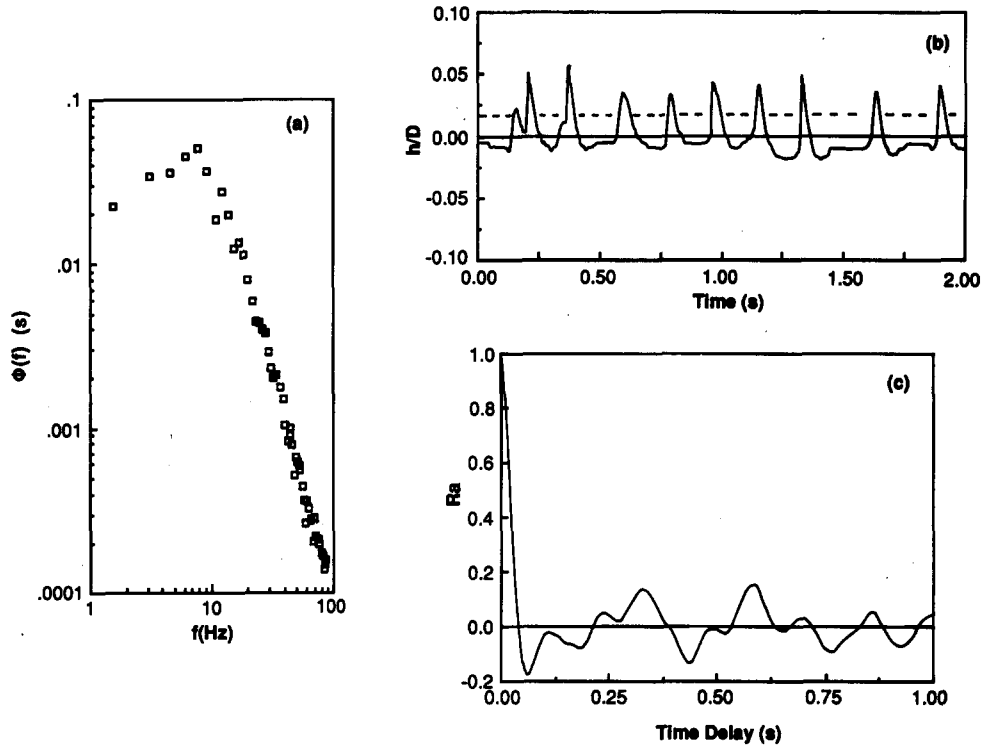

Figure 3. Wave spectrum (a), film thickness tracing around the mean thickness (b) and auto-correlation function (c) for $D = 9.53$ cm, $\mu_L = 80$ cP, $U_{LS} = 0.0033$ m/s and $U_{GS} = 14.4$ m/s.

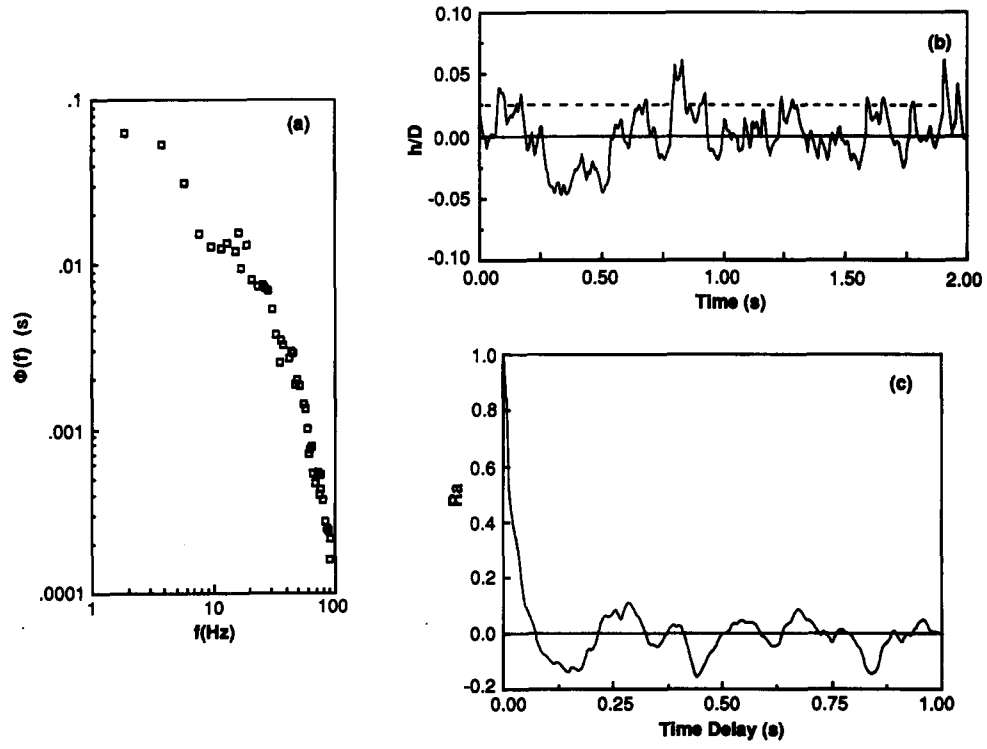

Figure 4. Wave spectrum (a), film thickness tracing around the mean thickness (b) and auto-correlation function (c) for $D = 9.53$ cm, $\mu_L = 1$ cP, $U_{LS} = 0.103$ m/s and $U_{GS} = 8.82$ m/s.

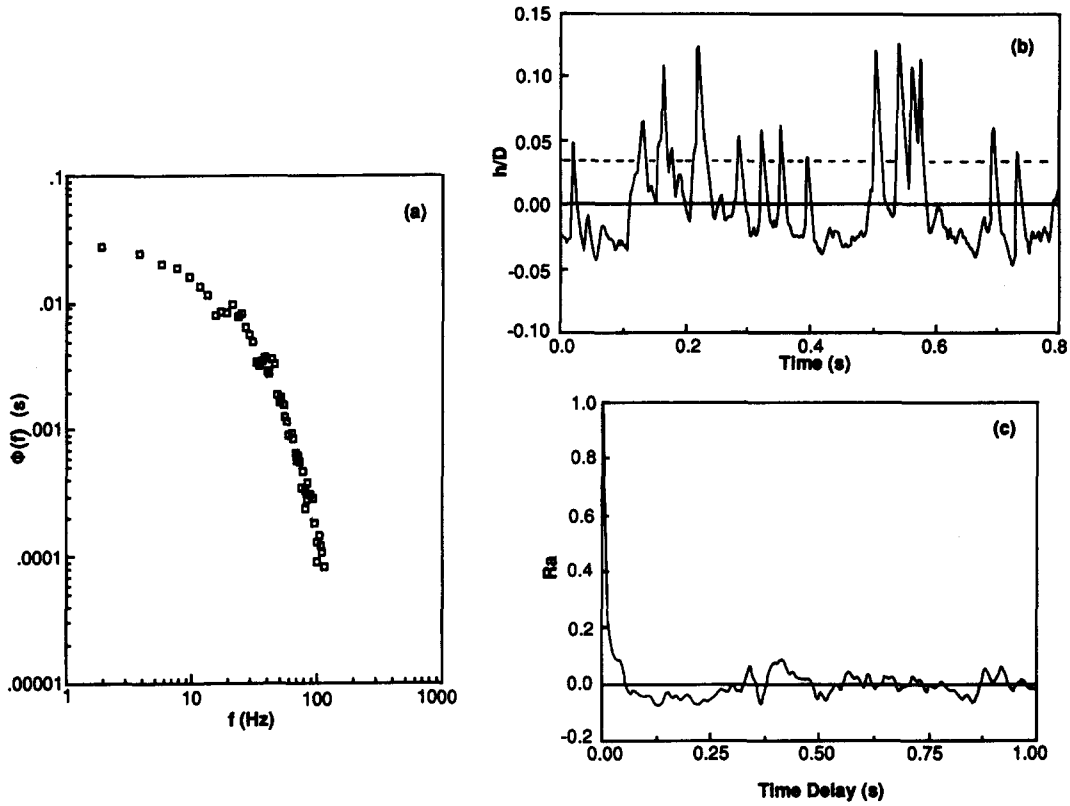

Figure 5. Wave spectrum (a), film thickness tracing aroung the mean thickness (b) and auto-correlation function (c) for $D = 2.52$ cm, $\mu_L = 1$ cP, $U_{LS} = 0.023$ m/s and $U_{GS} = 13.4$ m/s.

The wave height in the K–H and atomization regions is fairly insensitive to the gas velocity, despite the sharp decline of the mean and the base film thickness. The heights of the 2-D waves are usually lower than those of the K–H waves, with the exception of the heights of 2–D water waves on thick films. Although the gas velocity does not exert a significant influence on the wave amplitude, the latter is strongly affected by the liquid flow rate. For a 10-fold increase in the liquid velocity, the amplitude increases 3–5 times. This behavior has been associated with the theoretical prediction of steeper waves existing on thicker films (Bontozoglou & Hanratty 1989). Some other useful information can also be extracted from these data. The dimensionless wave amplitude, $\Delta h/D$, decreases with increasing pipe diameter, while all other parameters are kept constant, and it scales roughly with $D^{-0.5}$. There is also an effect of liquid viscosity on the wave amplitude when gas

Table 1. Wave properties for $D = 9.53$ cm and $\mu = 1$ cP

Type	U_{GS}(m/s)	U_{LS}(m/s)	h/D	$\Delta h/D$	$\Delta h/h$	C(m/s)	λ(cm)	Flatness	f_i/f_G
2-D	8.65	0.0095	0.072	0.017	0.24	0.59	2.5	3.1	3.0
K–H	13.49	0.0095	0.045	0.017	0.38	0.71	2.6	3.0	4.0
2-D	4.40	0.0244	0.191	0.028	0.15	0.48	5.8	2.4	1.9
2-D/K–H	6.79	0.0241	0.132	0.025	0.19	0.51	3.4	2.5	3.0
K–H	9.16	0.0240	0.101	0.031	0.31	0.70	3.9	3.5	4.0
K–H	12.46	0.0245	0.078	0.040	0.51	0.95	4.3	4.5	5.4
2-D	3.53	0.0581	0.303	0.059	0.19	0.61	12.1	2.7	2.8
2-D	4.29	0.0581	0.284	0.061	0.21	0.65	7.2	2.6	2.8
K–H	7.09	0.0581	0.186	0.057	0.31	0.78	7.8	3.7	3.5
K–H	9.22	0.0581	0.153	0.052	0.34	0.93	7.1	3.5	5.4
Atom.	14.11	0.0594	0.106	0.054	0.51	1.24	5.0	2.7	7.5
2-D	3.41	0.1050	0.364	0.090	0.25	0.79	16.8	2.9	3.5
2-D	4.42	0.1040	0.322	0.088	0.27	0.79	14.5	2.6	3.7
K–H	6.72	0.1040	0.248	0.083	0.34	0.95	10.8	4.2	5.6
K–H	8.82	0.1030	0.207	0.074	0.36	1.11	7.9	3.2	6.2
Atom.	14.36	0.1070	0.137	0.071	0.52	1.48	6.7	3.0	8.4

Table 2. Wave properties for $D = 9.53$ cm and $\mu = 80$ cP

Type	U_{GS}(m/s)	U_{LS}(m/s)	h/D	$\Delta h/D$	$\Delta h/h$	C(m/s)	λ(cm)	Flatness	f_i/f_G
K–H	8.55	0.0017	0.135	0.030	0.22	0.38	25.5	24.2	4.9
Atom.	12.96	0.0015	0.050	0.038	0.76	0.41	6.3	4.8	7.5
Atom.	16.19	0.0012	0.032	0.028	0.87	0.58	6.4	4.0	11.5
K–H	8.87	0.0052	0.125	0.045	0.36	0.43	19.9	8.9	7.0
Atom.	11.86	0.0033	0.081	0.044	0.54	0.43	7.8	4.3	7.4
Atom.	14.34	0.0033	0.074	0.045	0.60	0.67	8.0	3.0	8.3
Atom.	18.41	0.0033	0.043	0.034	0.78	0.74	4.1	3.2	11.6
K–H	7.36	0.0204	0.263	0.076	0.29	0.50	12.6	6.9	6.3
K–H	8.53	0.0185	0.237	0.082	0.35	0.51	7.3	3.9	7.0
Atom.	10.70	0.0201	0.191	0.066	0.35	0.55	5.6	3.5	7.8
Atom.	14.04	0.0189	0.142	0.065	0.46	0.67	5.3	4.8	8.6
Atom.	17.96	0.0198	0.133	0.059	0.52	0.78	3.4	2.8	11.0

velocity, pipe diameter and film height are kept constant. In general, the wave amplitudes for the more viscous liquids are 20–30% lower than those for water.

Experimental data on wave speed as a function of gas velocity are presented in figures 6 and 7 in two different ways. As a rule, the wave speed increases with increasing gas and liquid flow rates. The relative wave velocity, C/U_L, tends to unity as the gas rate increases (figure 6). This trend is also predicted from the linear theory by Andritsos & Hanratty (1987a), which is presented for two liquid viscosities. Here, C is the wave velocity as estimated from the cross-correlation functions and U_L is the actual liquid velocity based on the mean film thickness. Two groups of data are clearly identified. One group refers to the water and the other is associated with liquid viscosities >10 cP. The trends and the values of relative wave velocities in the first group are in close agreement with the data reported by Tsiklauri *et al.* (1979), which are taken with water in a 1.5×7.5 cm horizontal channel. As one may expect, relative wave velocities for viscous liquids are much higher than those for water, as illustrated in figure 6. Even a value of 20 was calculated for waves on a thin film in the 2.52 cm pipe and for a 70 cP liquid.

In figure 7, wave velocity data are plotted as a function of gas velocity. The wave speed increases monotonically with gas velocity in the K–H and atomization regions for a certain liquid rate, while from the limited number of data it seems that the wave velocity is not affected by the gas rate in the 2-D region. The data for liquid viscosities of 16 and 70 cP agree well with the data by Jurman *et al.* (1989) for the flow of glycerine–water solutions (viscosities 10–20 cP) in a 2.54 cm high horizontal channel. Not only are the trends identical in both investigations, but also the measured wave velocities are close, provided they are compared for similar gas velocities.

The wavelength of the 2-D waves range between 2–4 cm, with the exception of those on thick films. This range of wavelengths is predicted from linear stability theory. Nevertheless, at the point where the first K–H waves are observed the wavelength acquires its maximum value, to decrease

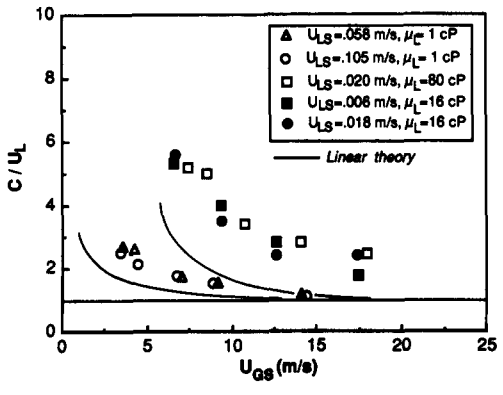

Figure 6. Relative wave velocity as a function of gas flow rate (open symbols are for the 9.53 cm pipe and closed symbols are for the 2.52 cm pipe, while the linear theory curves correspond to the conditions of open circle and open square).

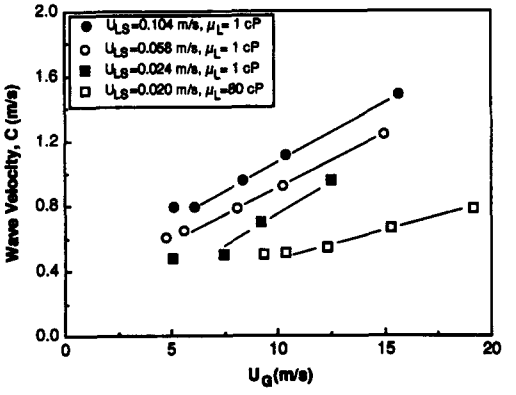

Figure 7. Effect of gas and liquid flow rate on the wave velocity.

subsequently with increasing gas velocity to a range of 2–4 cm. It should be added here that even for a 80 cP liquid the first disturbances are 2-D waves with wavelengths in good agreement with the linear theory by Andritsos & Hanratty (1987a). However, they quickly evolve to the large irregular waves depicted in the time traces.

The flatness factor, which is an expression of how peaky a process is, follows the behavior of the wavelength. Its value is 3 for the symmetrical and periodic 2-D waves, reaches a maximum value sharply at the initiation of the K–H waves and finally tends to values close to 3 for high gas velocities.

A detailed discussion on the interfacial friction factor and how it is influenced by the presence of waves can be found in Andritsos & Hanratty (1987b). It is noted that this quantity roughly scales with $\lambda/\Delta h$ and a discontinuity of its experimental value is observed after the inception of K–H waves.

CONCLUDING REMARKS

Using statistical analysis of film thickness traces, it is possible to verify the visually observed different nature of 2-D and K–H waves. The 2-D waves are periodic and uniform waves, which maintain their identity for several wave periods. In contrast, the K–H waves and those encountered in the atomization region are characterized by randomness, depicted in the film traces and in certain wave characteristics, as the auto- and cross-correlation functions. These waves are also characterized by strong wave–wave interactions and by the tendency to change their shape as they travel along the pipeline. Although almost all wave quantities are affected by the gas rate, no apparent change in the nature of waves seems to occur at the transition to the atomization region. It is argued that the atomization process starts with the formation of the K–H waves. However, due to kinetic energy considerations, either filaments are not torn off from the wave crests (except for thick films and consequently for large-amplitude waves) or the generated droplets do not travel long and high enough to hit the pipe wall, and especially the top of the pipe. It should be noted that conventionally the transition to atomization is defined when the first droplets hit the top of the pipe as the gas velocity increases, although the process of atomization starts at lower gas rates.

The calculations of a linear stability analysis predict fairly accurately the conditions of the wave inception and the wavelength and speed of the initial disturbances. As anticipated, any linear stability model fails to describe the wave characteristics away from the initiation point, as these are dominated by strong nonlinear interactions, such as wave splitting and wave coalescence.

Certainly, additional data are required to answer questions not clarified in this work. A direction in this aspect is the analysis of data taken at much shorter gas velocity intervals and the investigation of the evolution and coherence of the waves by a system of probes, spanning a large length of the pipe.

Acknowledgement—The author is indebted to Professor T. J. Hanratty for his guidance during the years this work was carried out.

REFERENCES

ANDRITSOS, N. 1986 Effect of pipe diameter and liquid viscosity on horizontal stratified flow. Ph.D. Thesis, Univ. of Illinois, Urbana.

ANDRITSOS, N. & HANRATTY, T. J. 1987a Interfacial instabilities for horizontal gas–liquid flows in pipelines. *Int. J. Multiphase Flow* **13,** 583–603.

ANDRITSOS, N. & HANRATTY, T. J. 1987b Influence of interfacial waves on hold-up and frictional pressure drop in stratified gas–liquid flows. *AIChE Jl* **33,** 444–454.

ANDRITSOS, N., WILLIAMS, L. & HANRATTY, T. J. 1989 Effect of liquid viscosity on the stratified–slug transition in horizontal pipe flow. *Int. J. Multiphase Flow* **15,** 877–892.

BENDAT, J. S. & PIERSOL, A. G. 1971 *Random Data: Analysis and Measurement Procedures.* Wiley-Interscience, New York.

BONTOZOGLOU, V. & HANRATTY, T. J. 1989 Wave height estimation in stratified gas–liquid flows. *AIChE Jl* **35**, 1346–1350.

BRUNO, K. & MCCREADY, M. J. 1988 Origin of roll waves in horizontal gas–liquid flows. *AIChE Jl* **34**, 1431–1440.

HANRATTY, T. J. 1983 Interfacial instabilities caused by the air flow over a thin liquid layer. In *Waves on Fluid Interfaces* (Edited by MEYER, R. E.), pp. 221–259. Academic Press, New York.

JURMAN, L. A., BRUNO, K. & MCCREADY, M. J. 1989 Periodic and solitary waves on thin, horizontal, gas-sheared liquid films. *Int. J. Multiphase Flow* **15**, 371–384.

TATTERSON, D. F., DALLMAN, J. C. & HANRATTY, T. J. 1977 Drop sizes in annular gas–liquid flows. *AIChE Jl* **23**, 68–76.

TSIKLAURI, G. V., BESFAMINILY, P. V. & BARYSHEV, YU. V. 1979 Experimental study of hydrodynamic processes for wavy water film in a cocurrent air flow. In *Two-phase Momentum, Heat and Mass Transfer* (Edited by DURST, F., TSIKLAURI, G. V. & AFGAN, N. H.), Vol. 1, pp. 357–372. Hemisphere, New York.